

Mesoscale Self-Assembly: Capillary Bonds and Negative Menisci

Ned Bowden, Scott R. J. Oliver, and George M. Whitesides*

Department of Chemistry and Chemical Biology, Harvard University, 12 Oxford St., Cambridge, Massachusetts 02138

Received: September 2, 1999

This paper describes the self-assembly of hexagonal plates (with 2.7 mm wide sides) at the interface between perfluorodecalin (PFD) and water. All 14 different hexagons that can be made by permuting the number and location of the hydrophobic and hydrophilic faces were examined. The plates attracted one another by lateral capillary forces involving the menisci on the hydrophilic faces. The plates were made of poly(dimethylsiloxane) (PDMS) containing aluminum oxide and had a density of 1.86 g/cm³, close to the density of PFD ($\rho = 1.91$ g/cm³). This work complements a previous paper (Bowden, N.; Choi, I. S.; Grzybowski, B. A.; Whitesides, G. M. *J. Am. Chem. Soc.* **1999**, *121*, 5373) that examined the self-assembly of hexagonal plates of PDMS ($\rho = 1.05$ g/cm³) that had a density close to that of water, and were attracted through menisci on the hydrophobic faces. The arrays that formed from the heavy ($\rho = 1.86$ g/cm³) hexagons with a particular pattern of *hydrophilic* faces were analogous to the arrays that formed from the light ($\rho = 1.05$ g/cm³) hexagons with that pattern of *hydrophobic* faces.

Introduction

This paper describes the self-assembly of small hexagonal plates composed of poly(dimethylsiloxane) (PDMS; $\rho = 1.05$ g/cm³) containing Al₂O₃ sufficient to increase their density to $\rho = 1.86$ g/cm³, floating at the interface between perfluorodecalin (PFD; $\rho = 1.91$ g/cm³) and H₂O ($\rho = 1.00$ g/cm³). We have examined the assembly of all 14 different hexagonal plates (which we will call “heavy” hexagons, $\rho = 1.86$ g/cm³, to distinguish them from unfilled or “light” hexagons of PDMS without additives, $\rho = 1.05$ g/cm³) that can be made by permuting the number and position of the hydrophobic and hydrophilic faces. These heavy hexagons assembled into ordered arrays through interactions between menisci of water on the *hydrophilic* faces. A previous paper has described the corresponding self-assembly of the 14 light hexagons; these hexagons interacted primarily through the menisci of PFD on the *hydrophobic* faces.¹

The work described in this paper represents part of our initial studies in the area of mesoscale self-assembly (MESA).^{1–11} In MESA, objects self-assemble into ordered arrays or aggregates through noncovalent forces; objects can be as small as several nanometers (colloids) to as large as thousands of kilometers (planets and stars).^{1,7,12} In MESA, we extend concepts from molecular biology and molecular self-assembly to the mesoscopic range of sizes.^{13–18} Molecular self-assembly is an active area of research with many accomplishments, but it is focused on assembly of molecules with nanometer sizes. Methods that extend self-assembly from molecules with nanometer sizes to nonmolecular objects with sizes of tens of nanometers and more would be welcome as potential approaches to new types of materials and new methods of fabrication and assembly.

There are many examples of spherical or quasispherical objects (from nanometer-sized colloids through micrometer-sized latex beads and millimeter-sized polyhedral objects) that self-assemble into ordered arrays; most of these arrays have been close-packed.^{19–44} We use nonspherical objects and directional forces to provide a higher degree of control of the self-assembly process. We have worked primarily with millimeter-sized objects

because they are easy to fabricate and characterize and the arrays produced can be quickly analyzed. The ideas and methods that are successful on the millimeter scale can be extended to the nm- and μ m-scale.^{20,22,23,25} This work has been extended to assembling objects in three dimensions using capillary forces.^{3,6,8,9}

MESA is an interesting field for several reasons. (i) MESA offers a way of generating arrays that are difficult or impossible to assemble otherwise. We believe that MESA will find uses in the assembly of electrical components, photonic band gap materials, membranes, and microelectromechanical systems (MEMs). (ii) MESA is an additive process (material is added to the array rather than removed, as is common in microfabrication of electronic devices). It is also error-correcting, and a type of precision assembly. (iii) The parameters that affect self-assembly are easily controlled. We can therefore study how each parameter affects the outcome of the assembly. (iv) MESA can serve as a physical realization of lattice models sometimes used to model biological systems (e.g., protein–ligand and DNA–DNA interactions).⁴

Our objective in this work was to test the hypothesis that the structures of the arrays that assembled from *light* hexagons interacting through menisci on a particular configuration of *hydrophobic* faces would be similar to the arrays that assembled from *heavy* hexagons interacting through menisci on the same configuration of *hydrophilic* faces. By changing the density of the hexagons from slightly more dense (1.05 g/cm³) than water to slightly less dense (1.86 g/cm³) than PFD, and by interchanging the hydrophobic and hydrophilic faces, we expected that we would generate sets of menisci on heavy hexagons with a particular configuration of hydrophobic and hydrophilic faces (that is, of positive and negative menisci) that were similar to the sets of menisci on the light hexagons with the positive and negative menisci interchanged (Figure 1).^{20,22,23} Because of the similarity on the heavy and light hexagons of the menisci with the hydrophobic and hydrophilic faces switched, we expect the heavy hexagons to assemble into arrays analogous to the arrays the light hexagons assembled into. This paper describes the assembly of the 14 different hexagons that can be made by

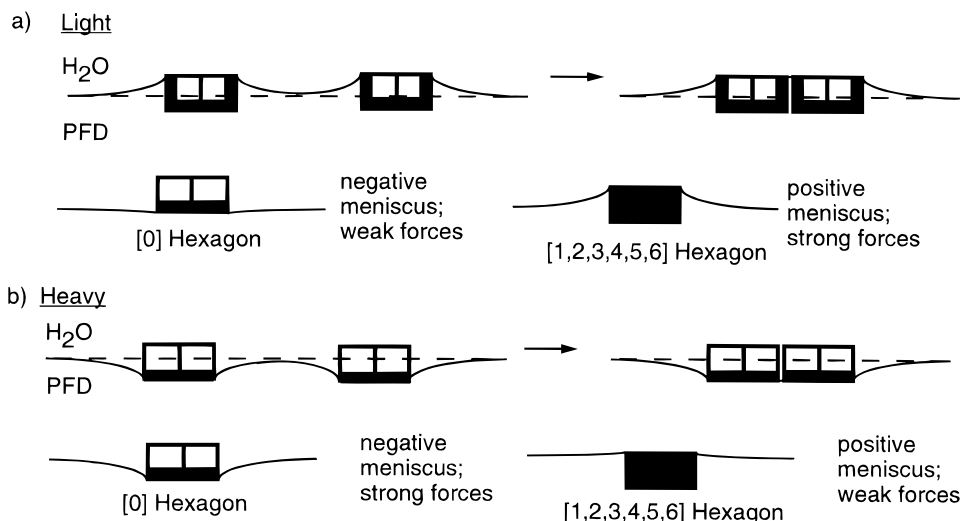


Figure 1. (a) The light hexagons ($\rho = 1.05 \text{ g/cm}^3$) are attracted by capillary forces through positive menisci; these hexagons are pulled into the interface by vertical capillary forces. The strength of the capillary forces depends on the density of the hexagons and the pattern of hydrophobic and hydrophilic faces. The light [0] hexagons barely perturb the interface and interact weakly. The light [1,2,3,4,5,6] hexagons have large positive menisci and interact strongly. (b) The heavy hexagons ($\rho = 1.86 \text{ g/cm}^3$) are attracted by capillary forces through negative menisci; these hexagons are pulled out of the interface by vertical capillary forces. The heavy [0] hexagons have large negative menisci and interact strongly. The heavy [1,2,3,4,5,6] hexagons barely perturb the interface and interact weakly. The thick lines and dark faces indicate hydrophobic faces; the thin lines indicate hydrophilic faces. The dotted lines show the level of the PFD/H₂O interface far from the objects.

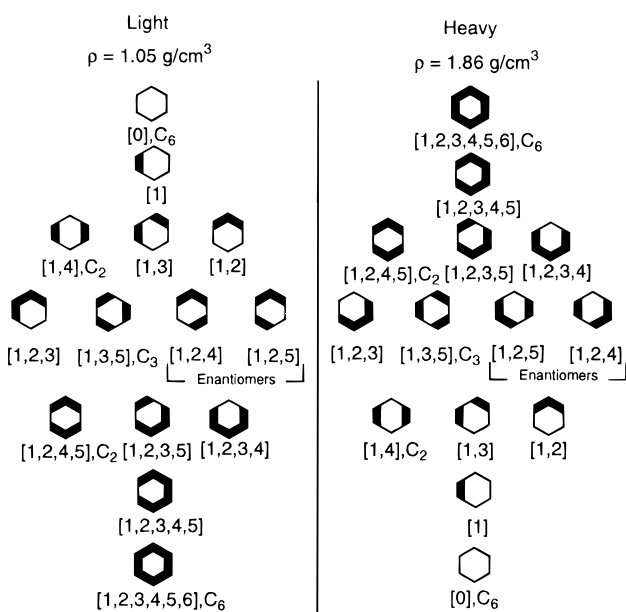


Figure 2. The 14 different hexagons that can be made by permuting the hydrophobic and hydrophilic faces on both light and heavy hexagons. The thick lines indicate hydrophobic faces; the thin lines indicate hydrophilic faces. We note the presence of a C_n axis of symmetry perpendicular to the hexagonal face. Hexagons with a C_n ($n > 1$) axis have a symmetric distribution of hydrophilic faces and float parallel to the interface. We postulate (and demonstrate) that the heavy hexagons form the same types of arrays as will light hexagons with the pattern of hydrophobic and hydrophilic faces interchanged (e.g., the light [1] hexagons and the heavy [1,2,3,4,5] hexagons).

permuting the hydrophobic and hydrophilic faces and compares structures formed on self-assembly of each of these heavy hexagons with the structures formed on self-assembly of the light hexagons with interchanged patterns of hydrophobic and hydrophilic faces (that is, hydrophobic faces on light hexagons would correspond to hydrophilic faces on heavy hexagons; Figure 2). In general, this hypothesis is confirmed by the experimental data, albeit with instructive differences between light and heavy hexagons.

Nomenclature. As in previous papers, we label the hydrophobic faces as numbers in parentheses.¹ For example, a [1,2,3,4] hexagon has four adjacent faces that are hydrophobic; the other two faces are hydrophilic. When we discuss a hydrophobic face, we place the number of the face in square brackets (i.e., the [2] face of a [1,2,3,4] hexagon). When we discuss a hydrophilic face, we do not use brackets (i.e., the 5 face of a [1,2,3,4] hexagon). For all of the hexagons, the top hexagonal face is hydrophilic and the bottom hexagonal face is hydrophobic.

Capillary Forces for Menisci on Hydrophobic and Hydrophilic Faces of Heavy Hexagons. There are two types of menisci on the faces. We call menisci of PFD that wet the hydrophobic faces “positive” menisci; the PFD in the menisci is above the mean plane of the interface. We call menisci of H₂O that wet the hydrophilic faces “negative” menisci; the water in the menisci is below the mean plane of the interface (Figure 1).

The equations describing the capillary forces between the objects have two contributions to the energy: (i) the energy decreases when the area at the PFD/H₂O interface decreases; (ii) the energy decreases when the liquid in the menisci is released to return to the level of the interface.^{20,45,46} Each interface has a characteristic free energy that is higher than the bulk free energy of the liquid; the interfacial free energy of the PFD/H₂O interface is 0.050 J m^{-2} .⁴⁷ The formation of menisci increases the area at the interface and raises the energy of the system; when the menisci are eliminated (for example, when two faces with similar menisci approach one another) the free energy of the system is lowered. The formation of menisci raises the average height of the interface by either raising the PFD above the mean plane of the interface (for positive menisci) or lowering H₂O below the mean plane of the interface (for negative menisci). When menisci are eliminated, the liquid in the menisci is released, the mean level of the PFD/H₂O interface is lowered, and the gravitational energy of the system is lowered.

Positive and negative menisci are treated the same by the equations describing the capillary forces. Thus, two positive menisci interact as strongly as two negative menisci of similar

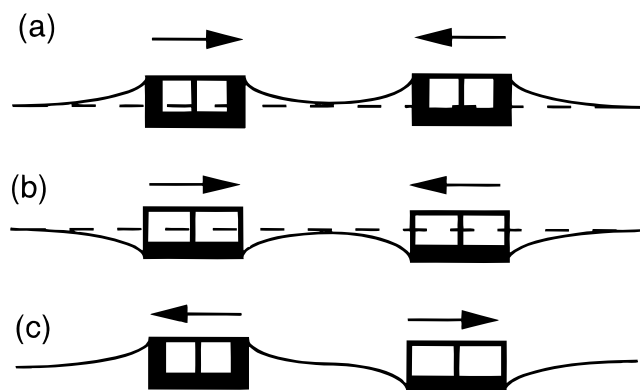


Figure 3. The three interactions between menisci at the interface. (a) A positive meniscus is attracted to a positive meniscus, and (b) a negative meniscus is attracted to a negative meniscus. (c) A positive meniscus is repelled by a negative meniscus. The thick lines indicate hydrophobic faces; thin lines indicate hydrophilic faces.

size and shape. It is because of this similarity that we expect the heavy hexagons to assemble through negative menisci into arrays analogous to those formed by the light hexagons through positive menisci.

The height of the menisci follow an exponential decay with a decay length of approximately 1.2 mm.¹ (The decay length is the distance from a face over which the height of the menisci decreases to 1/e or 36% of its maximum value.) Thus, faces that are in proximity, but not in contact, can interact through their menisci over distances of several millimeters.

We examined hexagons (2.7 mm on a face and 1.0–1.2 mm thick) with densities of 1.05 and 1.86 g/cm³. The hexagons with densities of 1.86 g/cm³ tended to float with their center of mass below the level of the PFD/H₂O interface far from the hexagons. For these hexagons, the positive menisci were small compared to the thickness of the hexagons, and the forces between two positive menisci were weak. The negative menisci were, in general, much larger than the positive menisci, and the forces between two negative menisci were strong (Figure 1b). These hexagons tended to assemble into arrays based on the interactions between the negative menisci. The hexagons with densities of 1.05 g/cm³ tended to float with their center of mass above the level of the interface far from the hexagons. For these hexagons, the heights of the negative menisci (relative to the mean plane of the PFD/H₂O interface) were small compared to the thickness of the hexagons, and the forces between two interacting negative menisci were weak. The positive menisci were, in general, much larger than the negative menisci, and the forces between two interacting positive menisci were strong (Figure 1a). These hexagons tended to assemble into arrays based on the interactions between the positive menisci.

For both light and heavy hexagons, the menisci follow the general rule that “like menisci attract, unlike menisci repel”. When two negative (or two positive) menisci approach one another, the area of the PFD/H₂O interface is decreased, the energy is lowered, and the objects come into contact (parts a and b of Figure 3). When a positive meniscus approaches a negative meniscus, the area of the PFD/H₂O interface is increased, the energy is increased, and the objects move away from one another (Figure 3c). The hexagons can approach one another from any angle; the faces move laterally with respect to one another to maximize the overlap of their menisci.

The form of the potential functions describing these interactions is not well understood due to limitations in our ability to model the menisci on arbitrary faces.^{1,2,20–25} Work by us and others on model systems (such as two infinitely long faces

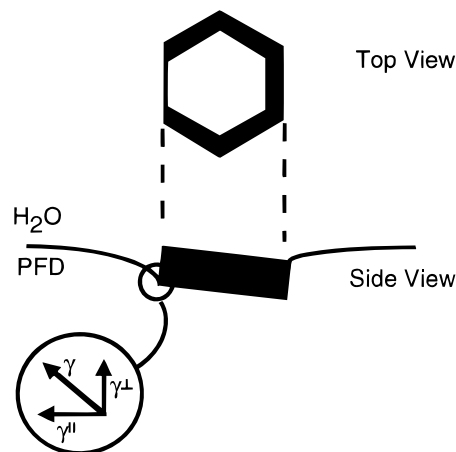


Figure 4. The surface tension, γ , can be broken into vertical, γ^\perp , and horizontal, γ^\parallel , components. The vertical component pulls the face into or out of the PFD/H₂O interface depending on the direction of the force.

interacting with one another or two cylinders interacting with one another) indicates that the energy of interaction between two negative menisci (or two positive menisci) decreases monotonically as they approach one another. Also, the energy of interaction between a positive meniscus and a negative meniscus increases monotonically as they approach one another. The case of a positive meniscus interacting with a negative meniscus is further complicated since we do not understand what happens to the contours of the menisci at very close separations (less than 1 mm); the menisci may start to dewet from the faces of the objects. Experimentally, an object with a negative meniscus repels an object with a positive meniscus at all separations; there does not appear to be an energy barrier to overcome, instead the energy appears to increase as the separation between the menisci decreases. We do not know the form of the potential energy functions for these interactions; we are only able to generalize about interactions between menisci.

Comparison Between Arrays Assembled from Light Hexagons ($\rho = 1.05$ g/cm³) and Heavy Hexagons ($\rho = 1.86$ g/cm³). The arrays that assembled from the light hexagons have been described in detail.¹ In this paper, we report the arrays that assembled from the heavy hexagons and we compare the arrays that assembled from the light and heavy hexagons (Figure 2). Pictures of arrays assembled from all of the different types of heavy and light hexagons are included in the paper. The pictures show *representative* arrays in each assembly, not the most ordered arrays. Beneath each picture, we show a schematic of the arrays to show the pattern of the hydrophobic and hydrophilic faces on the hexagons. All of the hexagons had the same dimensions for the length of a face; the hexagons are not all the same size in the figures due to differences in cropping of the original optical micrographs. In some figures, the hexagons have dark and light faces; the dark faces are hydrophobic and the light faces are hydrophilic.

Noncentrosymmetric Hexagons are Tilted at the Interface. Hexagons with a noncentrosymmetric pattern of hydrophobic faces have a noncentrosymmetric patterns of vertical capillary forces (Figure 4). These hexagons are tilted with respect to the interface. Some hexagons are tilted far enough to largely bury a face or vertex into the interface. We measured the tilt angles of the heavy and light hexagons using a procedure described elsewhere (Table 1).¹ We emphasize that the light and heavy hexagons (with the hydrophobic and hydrophilic faces interchanged) are tilted at the same angle.

TABLE 1: Tilt Angles, α , for the 1.2 mm Thick Hexagons^a

$\rho = 1.05 \text{ g/cm}^3$		$\rho = 1.86 \text{ g/cm}^3$	
Hexagon	α ($^\circ$)	Hexagon	α ($^\circ$)
	7 ± 2		8 ± 2
	3 ± 1		3 ± 1
	14 ± 1		13 ± 2
	6 ± 2		7 ± 1
	15 ± 1		16 ± 2
	14 ± 1		13 ± 2
	9 ± 2		11 ± 2

^a The uncertainties were standard deviations of at least 25 measurements on different hexagons.

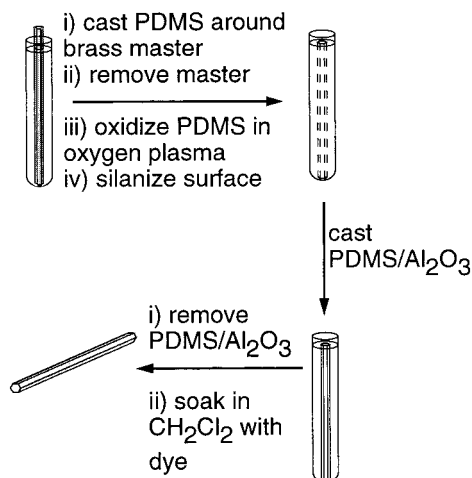


Figure 5. PDMS was cured around a brass hexagonal rod. The rod was removed from the cured PDMS leaving a hexagonal mold in the PDMS. The PDMS mold was oxidized in a plasma cleaner, and the surface of the oxidized PDMS was silanized with $\text{Cl}_3\text{SiCH}_2\text{CH}_2(\text{CF}_2)_5\text{CF}_3$ (United Chemical Technologies). PDMS with Al_2O_3 dispersed in it was added to the mold and cured. The PDMS/ Al_2O_3 hexagonal rod was removed from the mold and dyed by soaking overnight in CH_2Cl_2 with Sudan red 7B or crystal violet.

Experimental Section

Fabrication of the Hexagons. The fabrication of the hexagons followed procedures described previously; here, we note three characteristics (Figure 5).¹ (i) The hexagons had edges that were 2.7 mm wide; the hexagons were between 1.0 and 1.2 mm thick. (ii) The density of the hexagons was adjusted by adding Al_2O_3 . We used 1.45 g of Al_2O_3 per 1.00 g of PDMS to fabricate the hexagonal rods with a density of 1.86 g/cm^3 . (iii) Selected faces of the hexagons were colored for some experiments using procedures described previously.¹ These hexagons were used to characterize the orientation of hexagons in the arrays unambiguously, especially the partly ordered and disordered arrays.

The faces were made hydrophilic by oxidation in a plasma cleaner (5 min at medium on a Harrick PDC-23G).^{48,49} Faces that were to remain hydrophobic were protected from oxidation

by coating the faces with a thick layer of PDMS. In previous work, tape was used to protect the faces on the light hexagons from oxidation. We observed that tape did not protect the faces on the heavy hexagons from oxidation as well as the PDMS coating, so a new method was used (Figure 6). After coating selected faces with a thick (approximately 1–5 mm thick) layer of PDMS, the hexagonal PDMS was oxidized in an oxygen plasma that rendered the exposed surfaces hydrophilic. The protective PDMS layer was removed by peeling from the faces after oxidation; these faces were hydrophobic. The ends of the rods were cut with a razor blade into individual hexagonal plates. The plates were placed at the PFD/ H_2O interface manually with tweezers.

Fabrication of Hexagons with a Thin Layer of PDMS on the Faces. For some experiments, we wished to have a thin layer of PDMS coating the hexagons. Two methods were used to fabricate hexagons with a PDMS coating. In one method, a long (8 cm) hexagonal rod of PDMS/ Al_2O_3 was dipped into uncured PDMS and hung in an oven at $60 \text{ }^\circ\text{C}$ to cure. Most of the PDMS dripped off of the rod; after curing, the PDMS coating was $70 \text{ }\mu\text{m}$ thick at the center of a face, and $5 \text{ }\mu\text{m}$ thick at the edge between faces. In the second method, PDMS was added to the inside of the hexagonal mold used to fabricate the rods. The molds were hung in the oven at $60 \text{ }^\circ\text{C}$ and the PDMS was allowed to drip out of them. The PDMS was cured until it was sticky and did not flow; the inside of the mold was coated with a thin layer of partially cured PDMS. Next, PDMS/ Al_2O_3 was added to the mold and cured. The PDMS was $5 \text{ }\mu\text{m}$ thick at the center of a face and $120 \text{ }\mu\text{m}$ thick at an edge between faces. Both of these hexagons had densities of 1.86 g/cm^3 , within the limits of our ability to measure the densities.

Agitation. The hexagons were agitated on an orbital shaker with a diameter of rotation of approximately 2.5 cm at a fixed frequency of rotation, ω (s^{-1}), in a clockwise direction when viewed from the top. The frequency of rotation could be adjusted for each assembly. Approximately 80–100 hexagons were used in each assembly. The hexagons were placed in a dish (14.5 cm in diameter) coated with PDMS to make it hydrophobic; 150 mL of PFD and 250 mL of H_2O were added. The dish was made hydrophobic to repel the hexagons (the positive meniscus on the dish repels the negative menisci on the hexagons) when they approached the edge of the dish. Each assembly was agitated for a period of time (typically 1 h at $\omega = 1.0\text{--}1.2 \text{ s}^{-1}$), the agitation was stopped, the dish was gently placed on a white background, and the arrays were photographed. The dish was placed on the orbital shaker, the hexagons were separated from the arrays with tweezers, and the dish was agitated again. Each set of hexagons was agitated at least 10 times, and each experiment was repeated at least once with a new set of hexagons (for a total of at least 20 assemblies for each type of hexagon).

The light and heavy hexagons responded differently to the agitation. The light hexagons aggregated in the center of the dish at all frequencies of agitation up to the highest ($\omega = 1.5 \text{ s}^{-1}$). Above $\omega = 1.5 \text{ s}^{-1}$, bubbles of PFD formed at the PFD/ H_2O interface and disrupted the assembly. The assemblies of the light hexagons were usually complete in 30–60 min at $\omega = 1.5 \text{ s}^{-1}$. The heavy hexagons aggregated primarily in the center of the dish at low rates of agitation ($\omega < 1.0 \text{ s}^{-1}$); at intermediate rates of agitation ($\omega = 1.0\text{--}1.2 \text{ s}^{-1}$), they aggregated both along the edge of the dish and at its center; at high rates of agitation ($\omega > 1.2 \text{ s}^{-1}$), they aggregated exclusively along the edge of the dish. The heavy hexagons aggregated along the edge of the dish at some rates of agitation because their

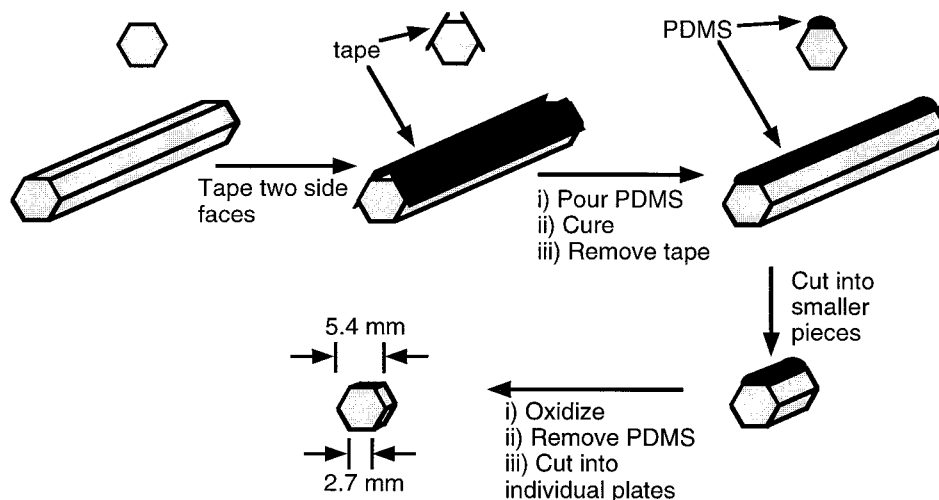


Figure 6. The 1 and 3 faces on long hexagonal rods of PDMS/Al₂O₃ were taped. PDMS was poured on the exposed face between the taped faces and cured. The tape was removed. The hexagonal rod was cut into smaller pieces (~5 mm in length). The rod was oxidized in a plasma cleaner, the PDMS coating was removed, and the ends of the rods were cut into individual hexagons. The hexagons were immediately placed at the PFD/H₂O interface.

TABLE 2: Advancing and Receding Contact Angles of PFD on PDMS and PDMS/Al₂O₃, Measured While Immersed in Water^a

PDMS	θ_a^{PFD} (deg)	θ_r^{PFD} (deg)
undyed PDMS	41	36
blue PDMS	51	41
red PDMS	62	42
undyed PDMS/Al ₂ O ₃	71	38
blue PDMS/Al ₂ O ₃	76	34
red PDMS/Al ₂ O ₃	75	32

^a The PDMS was dyed blue by soaking in CH₂Cl₂ with crystal violet overnight. The PDMS was dyed red by soaking in CH₂Cl₂ containing Sudan red 7B overnight.

density and mass are greater than that of the light hexagons. The heavy hexagons experienced higher centripetal forces than the light hexagons; these forces cause them to move along the edge of the dish at high rates of agitation.

The hexagons were not, in general, in contact with the dish; they tended to aggregate farther than 1 cm from the edge of the dish. Occasionally the arrays and individual hexagons collided with the wall of the dish; these collisions could break arrays apart. The hexagons along the edge of the dish were agitated by higher shear forces than the hexagons in the center of the dish and by collisions with the dish.

Contact Angles. We measured the contact angles of PFD under water (Table 2). To get reproducible results, we used flat slabs of PDMS. Briefly, we poured PDMS (with 1.45 g of Al₂O₃ per 1.00 g of PDMS dispersed in it) onto a silicon wafer in a Petri dish. The PDMS/Al₂O₃ was cured in an oven and removed. The PDMS/Al₂O₃ was left undyed, dyed in CH₂Cl₂ with crystal violet, or dyed in CH₂Cl₂ with Sudan red 7B. The PDMS/Al₂O₃ was washed with CH₂Cl₂ twice and dried in an oven (60 °C for 3 days) before measuring the contact angles.

Results and Discussion

Arrays of Heavy Hexagons Melt on Strong Agitation; Arrays of Light Hexagons Do Not. The arrays that assembled from the heavy hexagons “melted” at high rates of agitation. When ω reached a critical value, the arrays rapidly (~10 s) dissociated into individual hexagons. The melting happened at a sharply defined rate of agitation (± 0.1 s⁻¹) for each set of

hexagons (with the exception of the [0] hexagons). All of the hexagons melted at $\omega_m = 1.2$ – 1.3 s⁻¹, except the [0] hexagon which had a melting point range of $\omega_m = 0.7$ – 1.1 s⁻¹. At the low melting points ($\omega_m = 0.7$ s⁻¹), the [0] hexagons were agitated along the whole dish. The hexagons along the edge of the dish melted, but those in the center did not melt. At the high melting points ($\omega_m = 1.1$ s⁻¹), all of the [0] hexagons were distributed centrifugally along the edge of the dish and melted. We characterized the melting points of the open and closed arrays of the [1,4] hexagons. The open array melted at $\omega_m = 1.2$ s⁻¹; the closed array melted at $\omega_m = 1.3$ s⁻¹.


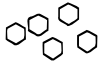



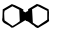







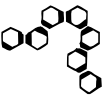







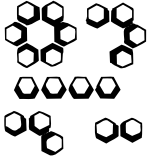

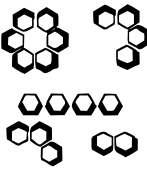















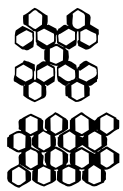

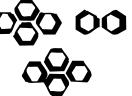







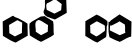

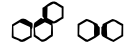


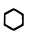

The light hexagons did not melt. The arrays formed from them were stable to the highest rates of agitation we could practically use ($\omega = 1.5$ s⁻¹); at higher values of ω , the systems began to form bubbles and drops of PFD at the PFD/H₂O interface and no longer gave useful results. The light hexagons did not melt because they remained in the center of the dish at all rates of agitation that we used; the shear forces were the weakest in the center of the dish. The heavy hexagons melted because they were agitated along the edge of the dish at high rates of agitation; the shear forces were strongest along the edge of the dish.

Ordered Arrays: [0], [1,4], [1,2], [1,3,5], [1,2,3,4], [1,2,4,5], and [1,2,3,4,5] Hexagons. These hexagons assembled into arrays that were similar to the arrays that assembled from the light hexagons; Table 3 and Figures 7, 8, 10, and 11 compare these sets of arrays. Three types of heavy hexagons, the [1,4], [1,2,3,4], and [1,2,3,4,5] hexagons, formed, in addition to the arrays predicted by analogy with those formed by the corresponding light hexagons, new structures not observed with the light hexagons.

[1,4] Hexagons. These hexagons assembled into a mixture of open and closed arrays at low rates of agitation ($\omega = 0.83$ s⁻¹; Figure 8b). As the agitation was increased, more hexagons assembled into closed arrays and fewer into open arrays; at $\omega = 1.2$ s⁻¹ only closed arrays formed (Figure 8c). Open arrays that were initially assembled at $\omega = 0.83$ s⁻¹ broke apart and reassembled into closed arrays at $\omega = 1.2$ s⁻¹. The closed arrays, once formed, were stable at all rates of agitation that we examined.

The preference for the open array at low rates of agitation depended on the stabilities of the two possible dimers that can

TABLE 3: Arrays Formed by the Light and Heavy Hexagons

$\rho = 1.05 \text{ g/cm}^3$			$\rho = 1.86 \text{ g/cm}^3$		
Hexagon	Array		Hexagon	Array	
		disordered aggregates due to weak interactions			disordered aggregates due to weak interactions
		dimers			dimers, trimers
		lines			lines
		kinked lines			kinked lines
		trimers			trimers, lines
		cyclic hexamers, dimers, trimers, tetramers, and lines			cyclic hexamers, dimers, trimers, tetramers, lines, and larger cyclic arrays
		open array			open array
		parallel lines			parallel lines
		parallel lines			parallel lines
		open array			open and closed array
		tetramers and dimers			tetramers and dimers
		lines			lines
		disordered aggregates with these two common assemblies			disordered aggregates with these two common assemblies
		closed array			closed array

be assembled by interactions between the hydrophilic faces (Figure 9). Two hexagons placed in the orientation that led to the closed array (the hexagons were manipulated manually with

tweezers) moved spontaneously relative to the one another (Figure 9a). Two hexagons placed in the orientation that led to the open array were stable (Figure 9b); this orientation was

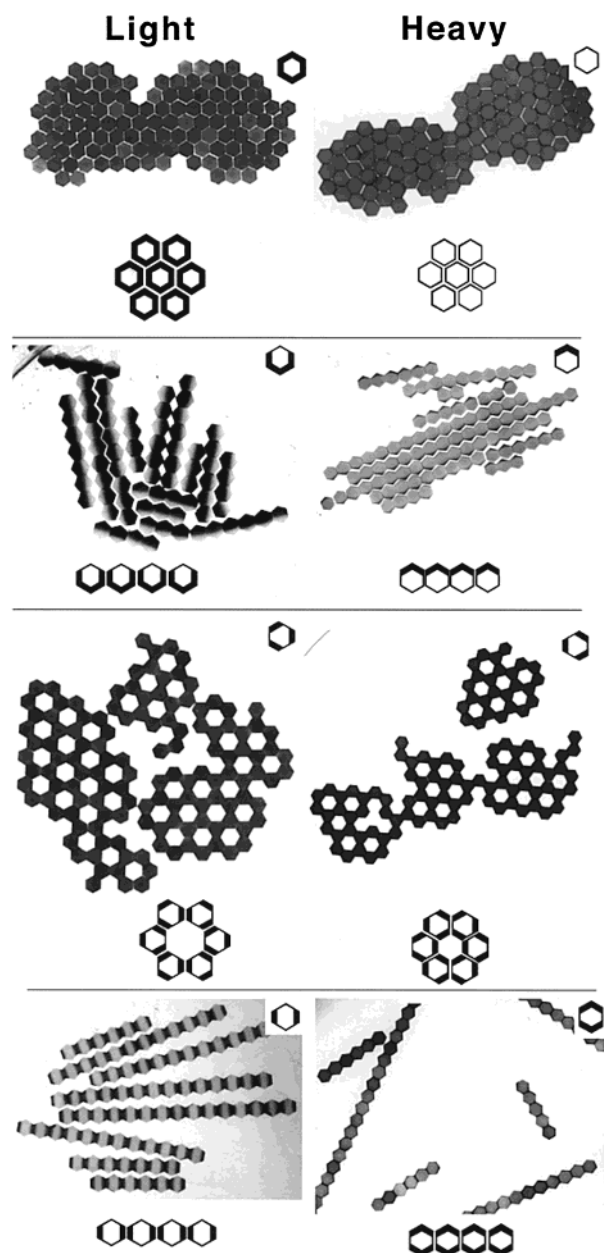


Figure 7. The ordered arrays formed from the heavy [0], [1,2], [1,3,5], and [1,2,4,5] hexagons and light [1,2,3,4,5,6], [1,2,3,4], [1,3,5], and [1,4] hexagons. The column on the right contains the heavy hexagons, the column on the left contains the light hexagons. Dark faces on the light [1,2,3,4] and [1,4] and heavy [1,2] hexagons indicate hydrophobic faces, and light faces indicate hydrophilic faces.

avored. We believe that the difference in stabilities of the dimers of the hexagons favored the open array; the extended array that ultimately formed was thus a kinetic product.

We believe that at high rates of agitation the shear forces favored the closed array. The open array was stable up to $\omega_m = 1.2 \text{ s}^{-1}$, but the closed array was stable at rates of agitation up to $\omega_m = 1.3 \text{ s}^{-1}$. There are at least two reasons why the closed array might be more stable than the open array. (i) The closed array packed more densely than the open array; there were more interactions between the hexagons in the closed than the open array. (ii) The closed array was stable when the hexagons moved slightly apart at high rates of agitation. At high rates of agitation, the arrays expanded and contracted; the closed array was stable but the open array was unstable to this agitation.

[1,2,3,4] Hexagons. These hexagons assembled predominately (90–100% of hexagons) into trimers (as predicted by analogy

with the light [1,2] hexagons) although 0–10% of the hexagons also formed lines (not predicted by analogy with the light [1,2] hexagons; Figure 10).

Why did the [1,2,3,4] hexagons occasionally assemble into lines? A possible explanation lies in their response to agitation. It is possible that the agitation momentarily changes the tilt of the hexagons with respect to the PFD/H₂O interface and make the negative menisci smaller and the positive menisci larger. The heavy hexagons assemble farther from the center of the dish than the light hexagons; this difference in location on the dish and the shear forces may temporarily alter the tilt of the hexagons. We do not understand how stable the tilts of the hexagons are at the interface over short periods of time (on the time frame of seconds), or how small changes in the tilt angle could affect the preference for the lines or trimers.

Another origin of the difference in behavior of heavy [1,2,3,4] and light [1,2] hexagons (and others) may lie in the difference in their wettability. We carried out four experiments to compare wettabilities of heavy and light hexagons. (i) We measured the contact angles of PFD under H₂O on these surfaces (Table 2). The advancing contact angle was higher for the PDMS with Al₂O₃ than for the PDMS without Al₂O₃. The heavy hexagons do not support the menisci of PFD as well as the light hexagons. (ii) We assembled white/undyed heavy hexagons that had a smaller advancing contact angle for the PFD than the blue or red heavy hexagons. The results of the assembly were the same as with the colored heavy hexagons. Thus, we wished to assemble hexagons that had faces with a lower contact angle of PFD on the hydrophobic faces that could be fabricated from only the PDMS/Al₂O₃ hexagonal rods. (iii) We removed the hexagons that had assembled into lines and placed them in a new dish with a fresh PFD/H₂O interface. Both dishes were agitated; and several hexagons that had assembled into trimers reassembled into lines in the original dish; the hexagons that had initially assembled into lines reassembled into trimers in the second dish. We repeated this experiment a number of times with the same results. These experiments demonstrated that the lines assembled from representative hexagons and were not due to a few defective hexagons. (iv) We used the hexagons that had a thin layer of PDMS on the faces (see the Experimental Section). These hexagons had the same contact angles for PFD and water as the light hexagons. These hexagons were patterned into [1,2,3,4] hexagons; both sets of hexagons assembled almost exclusively into *lines*. This experiment demonstrated that very small changes in the hexagonal plates can favor the lines over the trimers.

The differences in contact angles of PFD on the hydrophobic faces of the light and heavy hexagons could lead to the formation of some lines due to incomplete wetting of PFD on the hydrophobic faces. If the positive menisci slightly dewet from the [1] and [4] faces, the vertical capillary forces pushing the hexagons into the interface would be weakened, and thus the hydrophilic faces would be pushed out of the interface, and the size of the negative menisci on the hydrophilic faces would decrease.

We do not fully understand why a small number (0–10%) of the hexagons assembled into lines. From the experiments, it is clear that small changes in the hexagons have a large effect on the outcome of the assembly. We offer two possible explanations for the difference in the assembly of the heavy and light hexagons; we cannot determine what explanation is correct.

[1,2,3,4,5] Hexagons. These hexagons assembled into dimers and a few (<10% of the hexagons) trimers (Figure 11). Both

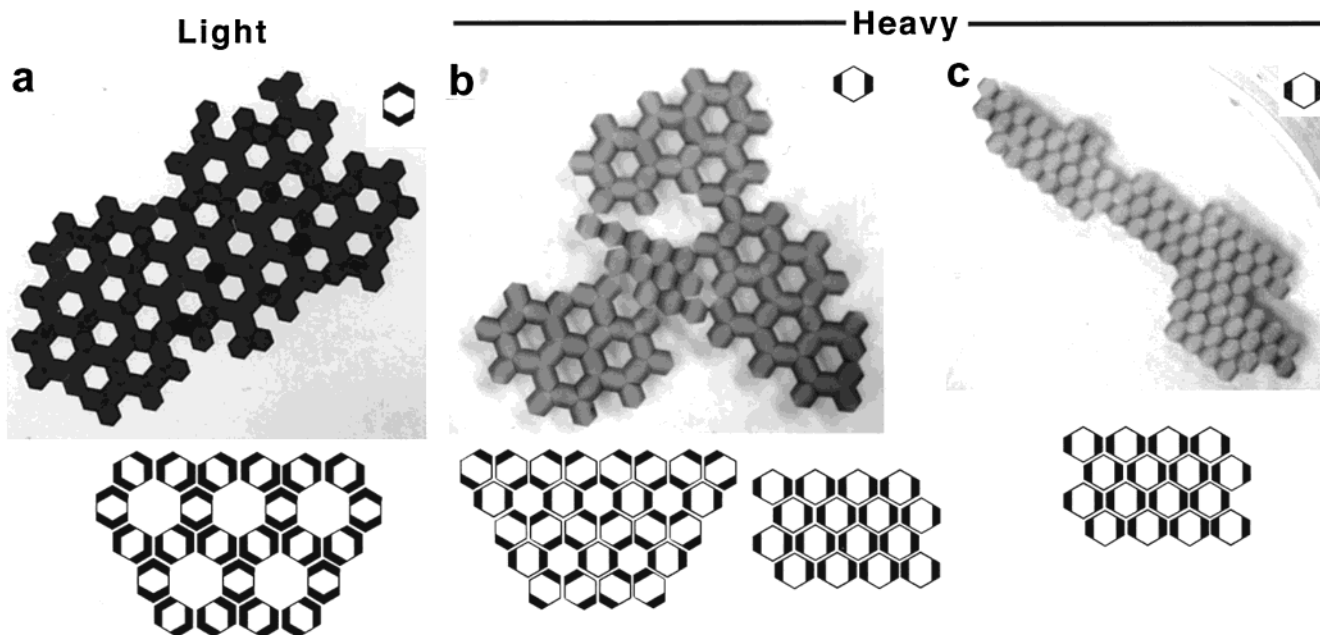


Figure 8. (a) The light [1,2,4,5] hexagons assembled exclusively into an open array. (b) The heavy [1,4] hexagons assembled into a mixture of open and closed arrays at low rates of agitation ($\omega = 0.83 \text{ s}^{-1}$). (c) At higher rates of agitation ($\omega = 1.2 \text{ s}^{-1}$) these hexagons assembled into closed arrays. The dark faces on the hexagons in (b) and (c) are the hydrophobic faces, the light faces are the hydrophilic faces.

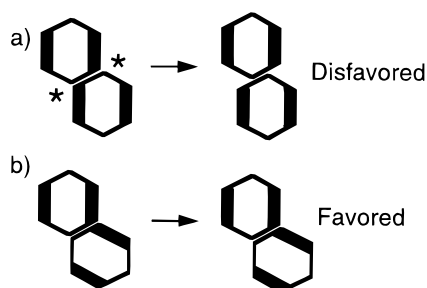


Figure 9. (a) Two heavy [1,4] hexagons were placed in this configuration by hand using tweezers; they spontaneously moved relative to one another due to the proximity of the positive and negative menisci (indicated by the stars) on the faces that were close but not in contact. The decay length of the menisci was approximately one-half the width of a face; faces that were close interacted through capillarity. This configuration of hexagons was disfavored at low rates of agitation. (b) Two heavy [1,4] hexagons were placed in this configuration by hand using tweezers. The faces that were close, but not in contact, had similar menisci. The hexagons did not move relative to one another. This configuration was favored at low rates of agitation.

arrays assembled through interactions between the 6 faces. The trimers assembled in the center of the dish where the agitation was the weakest, and the interacting faces were the hydrophilic faces.

Partly Ordered Arrays: [1,3], [1,2,4], [1,2,5], [1,2,3], and [1,2,3,5] Hexagons. These hexagons assembled as predicted based on analogy with the arrays that assembled from the light hexagons (Table 3; Figures 12 and 13). The structures of the arrays were the same for the analogous light and heavy hexagons.

[1,2,3] Hexagons. We noticed a difference in the assemblies of the light and heavy hexagons. The light hexagons assembled into dimers, trimers, tetramers, lines, and cyclic hexamers (Figure 13a). The heavy hexagons also assembled into arrays analogous to the light hexagons, and also formed more and larger cyclic arrays (Figure 13b).

The stability of the larger cyclic arrays is consistent with the capillary forces at the PFD/H₂O interface. We do know that

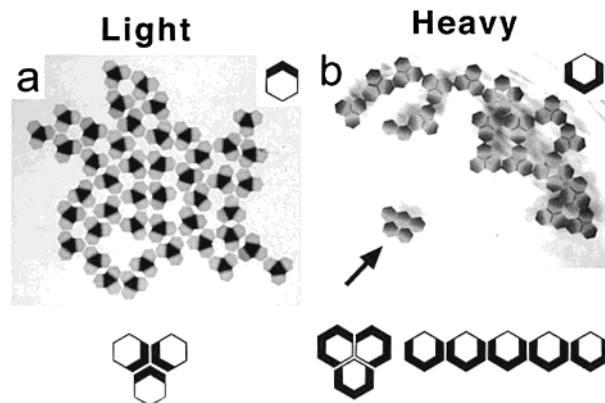


Figure 10. (a) The light [1,2] hexagons assembled exclusively into trimers. (b) The heavy [1,2,3,4] hexagons assembled into trimers and lines (indicated with an arrow).

the faces of the hexagons do not have to be in contact for a favorable interaction to exist, for example, the lines in Figure 13 interact through the vertices. The hexagons in the larger cyclic arrays, though not in contact, can still interact through capillarity because the decay length of the menisci is approximately 1.2 mm.

Disordered Arrays: [1] and [1,2,3,4,5,6] Hexagons. The assemblies formed by the [1] and [1,2,3,4,5,6] heavy hexagons were those predicted by analogy with the arrays of the light hexagons (Table 3 and Figure 14). The [1] hexagons assembled into disordered arrays with the two general trends for the assemblies as shown in Table 3. The [1,2,3,4,5,6] hexagons were pulled into the interface by gravity and the vertical capillary forces, and only small positive menisci were present. These menisci were too small, and the capillary forces associated with them too weak, to assemble the hexagons into ordered arrays.

Conclusions

The Heavy Hexagons Assembled into Arrays Analogous to those Formed by Light Hexagons with an Interchanged Pattern of Hydrophobic and Hydrophilic Faces. We have

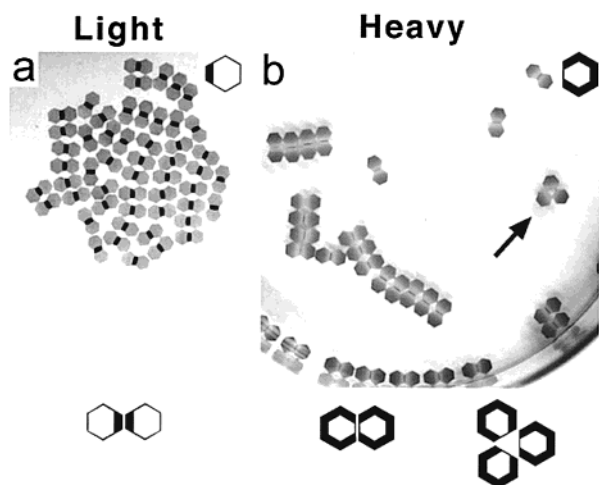


Figure 11. (a) The light [1] hexagons assembled exclusively into dimers. (b) The heavy [1,2,3,4,5] hexagons assembled into dimers and (<10%) trimers. The one trimer in the figure is indicated with an arrow.

demonstrated that the heavy and light hexagons having hydrophobic and hydrophilic faces self-assemble into arrays with analogous structures. For some hexagons we noticed small differences in the final arrays between analogous heavy and light hexagons. The origins of these differences are not clear, although they are largely understandable based on the differences in the contact angles of PFD on the faces of the heavy and light hexagons, and on the differences in the ways in which the heavy and light hexagons respond to the agitation (i.e., the heavy hexagons experience higher shear forces than the light hexagons, so arrays can be broken apart more easily for heavy than light hexagons). We tried to test these explanations by assembling hexagons with a thin (<120 μm thick) layer of PDMS on the heavy hexagons, removing the hexagons that did not assemble as predicted and placing them into a separate dish and agitating it, and assembling undyed heavy hexagons. It was not possible to estimate the relative importance of these two effects; small changes to the system could have large effects. Although there were small differences in the arrays of the heavy and light hexagons, the important and interesting aspects of the arrays were similar.

There are two significance aspects of this work. (i) It shows that objects can assemble using either positive or negative menisci, and with equal and high predictability. (ii) It demonstrates that it is possible to predict the structure of aggregates and outlines some of the parameters affecting self-assembly.

This study supports the hypothesis that self-assembly results from capillary interactions between menisci with matching contours. The arrays assembled in a way that juxtaposed faces on the heavy hexagons that matched the contours of the negative menisci; similar observations describe the patterns of aggregation of the light hexagons. The contours of the menisci provided directionality to the assembly; ordered arrays assembled based on these interactions.

The Melting Points Were Similar For All But the [0] Hexagons. The phase transition between ordered arrays and individual hexagons at the PFD/H₂O interface is an interesting phenomenon. It is related on some level to the solid to gas or liquid to gas phase change for molecules. The melting point for each type of hexagon was $\omega_m = 1.2\text{--}1.3 \text{ s}^{-1}$, except for the [0] hexagons which had a melting point range of $\omega_m = 0.7\text{--}1.1 \text{ s}^{-1}$. At the melting point, the hexagons were agitated along the edge of the dish so strongly that the capillary forces were too weak to keep the hexagons in contact. Because the

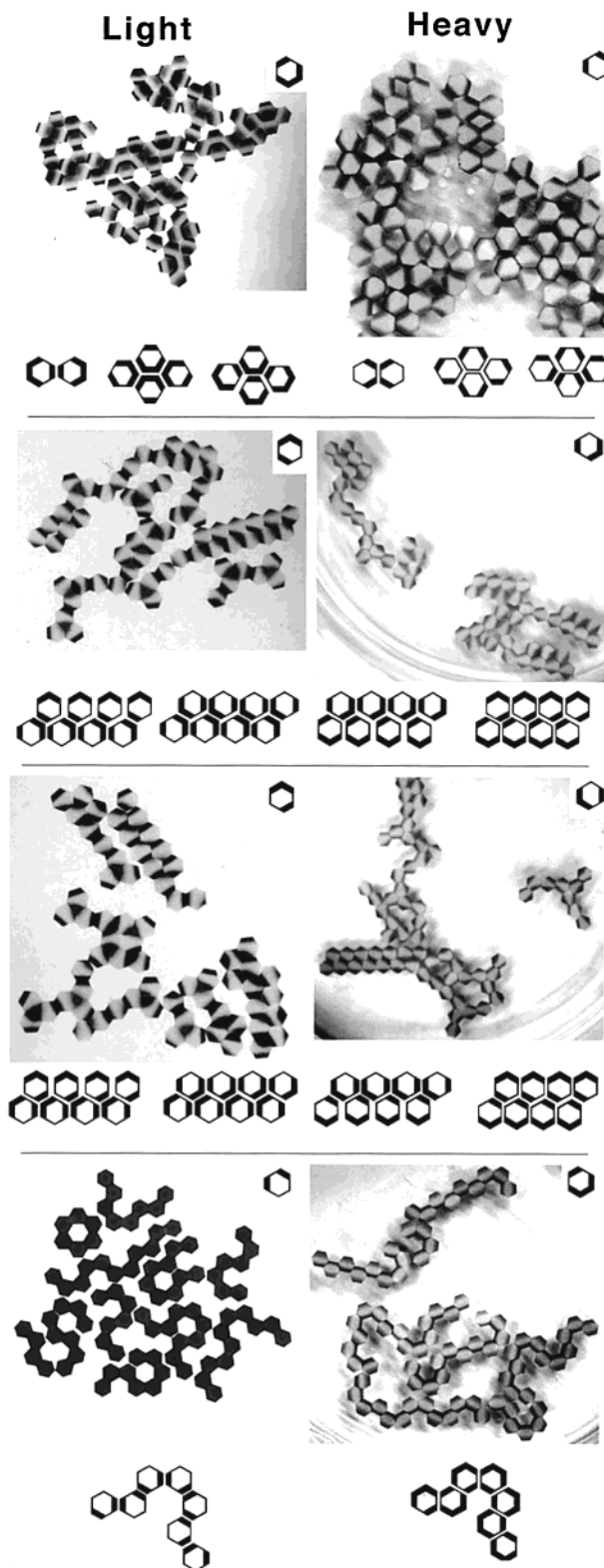


Figure 12. The arrays that assembled from the heavy [1,3], [1,2,4], [1,2,5], and [1,2,3,5] hexagons and the light [1,2,3,5], [1,2,5], [1,2,4], and [1,3] hexagons are shown. The right column contains the heavy hexagons and the left column contains the light hexagons.

light hexagons assembled only in the center of the dish, where the shear forces were weakest, they did not melt. It is noteworthy that the melting points were similar for a wide range of hexagons.

Acknowledgment. The authors thank Bartosz A. Grzybowski for helpful discussions. N.B. thanks the Department of

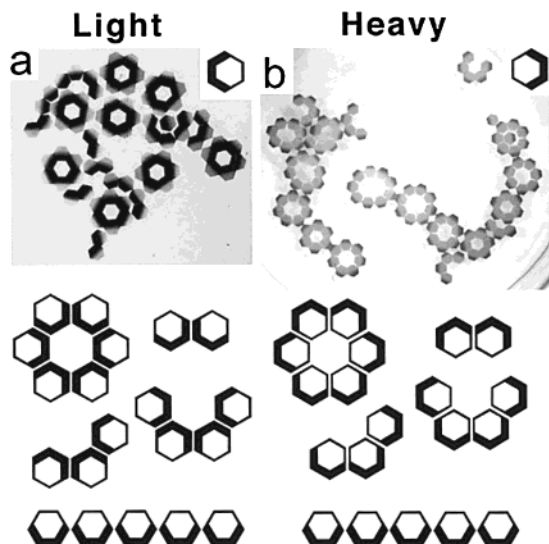


Figure 13. (a) The light [1,2,3] hexagons assemble into linear arrays, cyclic hexamers, dimers, trimers, and tetramers. (b) The heavy [1,2,3] hexagons assembled into arrays similar to those formed by the light [1,2,3] hexagons; the heavy [1,2,3] hexagons had a higher tendency than the light hexagons to assemble into cyclic arrays with more than six hexagons in the array.

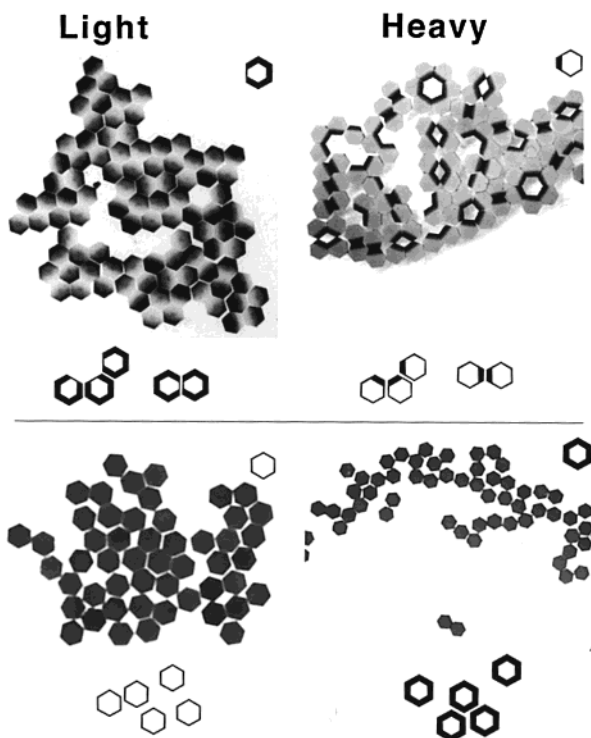


Figure 14. The arrays that assembled from the heavy [1] and [1,2,3,4,5,6] hexagons and the light [1,2,3,4,5] and [0] hexagons.

Defense for a pre-doctoral fellowship. This work was supported by the NSF (CHE-9901358 and Grant ECS8729405), NIH (Grant GM30367), and DARPA (SPAWAR and AFRL).

References and Notes

- (1) Bowden, N.; Choi, I. S.; Grzybowski, B.; Whitesides, G. M. *J. Am. Chem. Soc.* **1999**, *121*, 5373–5391.
- (2) Bowden, N.; Terfort, A.; Carbeck, J.; Whitesides, G. M. *Science* **1997**, *276*, 233–235.
- (3) Breen, T. L.; Tien, J.; Oliver, S. R. J.; Hadzic, T.; Whitesides, G. M. *Science* **1999**, *284*, 948–951.

- (4) Choi, I. S.; Bowden, N.; Whitesides, G. M. *J. Am. Chem. Soc.* **1999**, *121*, 1754–1755.
- (5) Choi, I. S.; Bowden, N. B.; Whitesides, G. M. *Angew. Chem., Int. Ed. Engl.* **1999**, *111*, 3265–3268.
- (6) Huck, W. T. S.; Tien, J.; Whitesides, G. M. *J. Am. Chem. Soc.* **1998**, *120*, 8267–8268.
- (7) Isaacs, L.; Chin, D. N.; Bowden, N.; Xia, Y.; Whitesides, G. M. *Self-assembling Systems on Scales from Nanometers to Millimeters: Design and Discovery*; Isaacs, L., Chin, D. N., Bowden, N., Xia, Y., Whitesides, G. M., Eds.; John Wiley & Sons Ltd: New York, 1999; Vol. 4, Chapter 1, pp 1–46.
- (8) Terfort, A.; Bowden, N.; Whitesides, G. M. *Nature* **1997**, *386*, 162–164.
- (9) Terfort, A.; Whitesides, G. M. *Adv. Mater.* **1998**, *10*, 470–473.
- (10) Tien, J.; Breen, T. L.; Whitesides, G. M. *J. Am. Chem. Soc.* **1998**, *120*, 12670–12671.
- (11) Wu, H.; Bowden, N.; Whitesides, G. M. *Appl. Phys. Lett.* **1999**, *75*, 3222–3224.
- (12) Mesoscale self-assembly is defined as the self-assembly of objects into ordered arrays or aggregates through noncovalent forces under equilibrium or steady-state conditions.
- (13) Desiraju, G. R. *Crystal Engineering: The Design of Organic Solids*; Elsevier: New York, 1989.
- (14) Poirier, G. E. *Chem. Rev.* **1997**, *97*, 1117–1127.
- (15) Bain, C. D.; Troughton, E. B.; Tao, Y.-T.; Evall, J.; Whitesides, G. M.; Nuzzo, R. G. *J. Am. Chem. Soc.* **1989**, *111*, 321–335.
- (16) Lehn, J.-M. *Angew. Chem., Int. Ed. Engl.* **1988**, *27*, 89–112.
- (17) Whitesides, G. M.; Mathias, J. P.; Seto, C. T. *Science* **1991**, *254*, 1312–1319.
- (18) Voet, D.; Voet, J. G. *Biochemistry*; John Wiley & Sons: New York, 1995.
- (19) Mirkin, C. A.; Letsinger, R. L.; Mucic, R. C.; Storhoff, J. J. *Nature* **1996**, *382*, 607–609.
- (20) Kralchevsky, P. A.; Paunov, V. N.; Denkov, N. D.; Ivanov, I. B.; Nagayama, K. *J. Colloid Interface Sci.* **1993**, *155*, 420–437.
- (21) Yamaki, M.; Higo, J.; Nagayama, K. *Langmuir* **1995**, *11*, 2975–2978.
- (22) Kralchevsky, P. A.; Nagayama, K. *Langmuir* **1994**, *10*, 23–36.
- (23) Nagayama, K.; Takeda, S.; Endo, S.; Yoshimura, H. *J. Appl. Phys.* **1995**, *34*, 3947–3954.
- (24) Lazarov, G. S.; Denkov, N. D.; Velev, O. D.; Kralchevsky, P. A.; Nagayama, K. *J. Chem. Soc., Faraday Trans.* **1994**, *90*, 2077–2083.
- (25) Israelachvili, J. *Intermolecular and Surface Forces*; Academic Press, Inc.: San Diego, 1992.
- (26) Elghanian, R.; Storhoff, J. J.; Mucic, R. C.; Letsinger, R. L.; Mirkin, C. A. *Science* **1997**, *277*, 1078–1080.
- (27) Alivisatos, A. P. *Endeavour* **1997**, *21*, 56–60.
- (28) Kolagunta, V. R.; Janes, D. B.; Bielefeld, J. D.; Andres, R. P.; Osifchin, R. G.; Henderson, J. I.; Kubiak, C. P. *Proc. Electrochem. Soc.* **1996**, *95*, 56–69.
- (29) Murray, C. B.; Kagan, C. R.; Bawendi, M. G. *Science* **1995**, *270*, 1335–1338.
- (30) Kim, E.; Whitesides, G. M. *Chem. Mater.* **1995**, *7*, 1257–1264.
- (31) Alivisatos, A. P.; Johnsson, K. P.; Peng, X.; Wilson, T. E.; Loweth, C. J.; Bruchez, M. P., Jr.; Schultz, P. G. *Nature* **1996**, *382*, 609–611.
- (32) Trau, M.; Sankaran, S.; Saville, D. A.; Aksay, I. A. *Langmuir* **1995**, *11*, 4665–4672.
- (33) Trau, M.; Saville, D. A.; Aksay, I. A. *Science* **1996**, *272*, 706–709.
- (34) Paunov, V. N.; Kralchevsky, P. A.; Denkov, N. D.; Nagayama, K. *J. Colloid Interface Sci.* **1993**, *157*, 100–112.
- (35) Velev, O. D.; Furusawa, K.; Nagayama, K. *Langmuir* **1996**, *12*, 2385–2391.
- (36) Weiss, J. A.; Oxtoby, D. W.; Grier, D. G.; Murray, C. A. *J. Chem. Phys.* **1995**, *103*, 1180–1190.
- (37) Murray, C. A.; Grier, D. G. *Annu. Rev. Phys. Chem.* **1996**, *47*, 421–462.
- (38) Park, S. H.; Qin, D.; Xia, Y. *Adv. Mater.* **1998**, *10*, 1028–1032.
- (39) Crocker, J. C.; Grier, D. G. *MRS Bull.* **1998**, *23*, 24–31.
- (40) Grier, D. G. *Nature* **1998**, *393*, 621.
- (41) Weiss, J. A.; Larsen, A. E.; Grier, D. G. *J. Chem. Phys.* **1998**, *109*, 8659–8666.
- (42) Adams, M.; Dogic, Z.; Keller, S. L.; Fraden, S. *Nature* **1998**, *393*, 349–351.
- (43) Burns, M. M.; Fournier, J. M.; Golovchenko, J. A. *Phys. Rev. Lett.* **1989**, *63*, 1233–1236.
- (44) Tu, J. K.; Talghader, J. J.; Hadley, M. A.; Smith, J. S. *Electron. Lett.* **1996**, *31*, 1448–1449.
- (45) Chan, D. Y. C.; Henry, J. D., Jr.; White, L. R. *J. Colloid Interface Sci.* **1981**, *79*, 410–418.

- (46) Gao, C. *Appl. Phys. Lett.* **1997**, *71*, 1801–1803.
- (47) Markina, Z. N.; Bovkun, O. P.; Zadymova, N. M.; Roskete, E.; Shchukin, E. D.; Makarov, K. N.; Gervits, L. L. *Zh. Vses. Khim. O-va. im. D. I. Mendeleeva* **1988**, *33*, 346–348.
- (48) Fakes, D. W.; Davies, M. C.; Browns, A.; Newton, J. M. *Surf. Interface Anal.* **1988**, *13*, 233.
- (49) Morra, M.; Occiello, E.; Marola, R.; Garbassi, F.; Humphrey, P.; Johnson, D. J. *Colloid Interface Sci.* **1990**, *137*, 11–24.